IOPscience iopscience.iop.org

Home Search Collections Journals About Contact us My IOPscience

Density functional study of collective electron localization: detection by persistent current

This article has been downloaded from IOPscience. Please scroll down to see the full text article.

2009 J. Phys.: Condens. Matter 21 155602

(http://iopscience.iop.org/0953-8984/21/15/155602)

View the table of contents for this issue, or go to the journal homepage for more

Download details:
IP Address: 129.252.86.83
The article was downloaded on 29/05/2010 at 19:07

Please note that terms and conditions apply.

J. Phys.: Condens. Matter **21** (2009) 155602 (8pp) doi:10.1088/0953-8984/21/15/155602

Density functional study of collective electron localization: detection by persistent current

Marc Siegmund, Markus Hofmann and Oleg Pankratov

Lehrstuhl für Theoretische Festkörperphysik, Universität Erlangen-Nürnberg, Staudtstrasse 7 B2, D-91058 Erlangen, Germany

E-mail: Siegmund@physik.uni-erlangen.de

Received 24 July 2008, in final form 19 February 2009
Published 20 March 2009
Online at stacks.iop.org/JPhysCM/21/155602

Abstract

We apply the optimized effective potential (OEP) implementation of density functional theory (DFT) to the model system of interacting spinless electrons on a quantum ring. The ring encircles a magnetic flux that induces a persistent current. In a perfect rotationally invariant system the current does not depend on the electron–electron interaction (the latter is characterized by a standard dimensionless parameter r_S) and hence is not sensitive to the microscopic structure of the electron correlated state. This changes, however, if a symmetry-breaking external potential is introduced or, in a realistic system, due to the crystal lattice potential (Hamer *et al* 1987 *J. Phys. A: Math. Gen.* **20** 5677–93). In our model, we calculate the persistent current as a function of r_S in the presence of a weak Gaussian-shaped 'impurity' potential. We find that while below a threshold value $r_S < r_S^c \approx 2.05$ the current is independent of r_S, it decays exponentially for $r_S > r_S^c$. This signals the formation of an electron Wigner crystal pinned by the impurity potential. The electron density, homogeneous below r_S^c, indeed shows a periodic modulation at $r_S > r_S^c$. The modulation amplitude follows a $(r_S - r_S^c)^{1/2}$ behaviour which is characteristic for a second-order phase transition, as expected in the mean-field-type DFT-OEP approach. Our calculation shows that the macroscopic current, which is a quantity directly accessible in DFT, can serve as an indicator of the formation of a correlated electron state.

(Some figures in this article are in colour only in the electronic version)

1. Introduction

Density functional theory (DFT) [1, 2] provides a basis for the vast majority of contemporary *ab initio* studies of many-particle quantum systems [3]. A decisive advantage of DFT which underlies its exceptional computational performance is that it casts the quantum many-body problem in terms of simple collective variables such as the particle density, the spin density (spin-density functional theory, SDFT) and the current density (current-density functional theory, CDFT). Originally introduced as a ground state theory [1, 2], DFT has been extended to time-dependent problems [4] and used for a description of the many-body response in linear [5] and non-linear [6, 7] regimes.

Although formally exact, DFT, when dealing with realistic systems, must rely on approximate exchange–correlation (xc) functionals $E_{xc}[n]$ that express the exchange–correlation energy of a system through the collective variables in use, e.g. the particle number density $n(\vec{r})$. Many approximations for $E_{xc}[n]$ have been developed, the most popular being the local density approximation (LDA) where the local functional $E_{xc}[n]$ is adopted. The accuracy of various approximations is very difficult to control. In special cases (e.g. the exactly solvable Hubbard-type model [8], the helium atom or two-electron ions which also allow an essentially exact solution [9]) the exact exchange–correlation potential v_{xc} can be constructed and compared with the approximate one. In this way the essential features of v_{xc} such as its discontinuity as a function of the particle number [8] and the large-distance asymptotic

 © 2009 IOP Publishing Ltd Printed in the UK

behaviour [9] can be verified. Although the output of a static DFT is, strictly speaking, limited to the particle density in the ground state $n_0(\vec{r})$ and the total ground state energy $E_0 = E[n_0(\vec{r})]$, its realm is often stretched beyond the validity limits. For example, the fictitious DFT–LDA band structures, which are the eigenvalue spectra of the auxiliary one-particle Kohn–Sham equations [2], typically provide an insight into a real excitation spectrum. This makes the one-particle LDA energy spectrum a useful starting point for the many-body calculations. Of course, the ability of an approximate xc functional to correctly reproduce the ground state is a prerequisite for these DFT extensions.

An interesting situation, also driving DFT to its limits, is the formation of a Wigner crystal [10] at low electron densities. Within DFT, this problem has been addressed for the two-dimensional electron gas [11] and for one-dimensional quantum wires [12]. The periodic density modulation was imposed by hand and the ground state energy was evaluated with the Fermi-liquid exchange–correlation functionals and the Thomas–Fermi–Weizsäcker approximation for the kinetic energy term. In two dimensions, the Wigner transition was found [11] at a critical value of r_S^c between 31 and 35, in good agreement with the value of $r_S^c = 37 \pm 5$ from quantum Monte Carlo simulations [13]. In the one-dimensional wire the transition was estimated at $r_S^c \approx 5.5$ [12], although the precise value was dependent on the details of the lateral confinement. Of course, a detailed description of the correlated state requires a knowledge of the correlation function. The latter is, however, beyond DFT formalism, where one has to rely on the less informative density distribution. The particle density can, indeed, reflect the Wigner crystal formation if the translational symmetry has been broken to prevent the crystal 'gliding'. Yet the density distribution alone does not allow us to distinguish the localized state from a delocalized one.

In this paper we pursue the idea of detecting the Wigner crystal by calculating the persistent current. We explore the simplest one-dimensional situation with electrons confined on a quantum ring which is threaded by a magnetic flux. To break the rotational invariance we introduce a very weak 'impurity' potential. Clearly, the vanishing localized potential does not affect tunnelling of individual electrons, but should suppress the current of the whole bundle of electrons building the Wigner crystal. In a realistic system, the symmetry breaking due to the crystal lattice potential also leads to an interaction dependence of the current [14]. Calculating the current as a function of r_S, we are able to identify the crystallization transition. At this point we want to make it clear that the choice of the ring geometry is dictated by calculational convenience. It is not the goal of this paper to address specific properties of correlated one-dimensional fermions (see below).

In the linear response regime the persistent current criterion is equivalent to the ground state curvature criterion (the second derivative of the ground state energy with respect to magnetic flux). The latter has been studied numerically for interacting one-dimensional fermions on a lattice [15], where multiple insulating phases due to umklapp-scattering driven instabilities were found. The occurrence of such phases in our case seems unlikely since our system is quasi-continuous (although artificially discretized due to the real space basis functions). The electron localization function (ELF) [16], which we calculated in parallel with the persistent current, does not provide any indications of multiple phases.

The ground state properties of quantum dots and rings [17] such as the addition energy, the chemical potential, the spontaneous spin magnetization and in particular the persistent current have been addressed with CDFT in LDA [18, 19]. The harmonic confining potential was chosen to keep electrons on a ring such that only the lowest transversal subband was occupied. Wigner crystallization, however, was not considered. Similar to the Mott–Hubbard insulator, the description of the Wigner crystal requires more sophisticated approximations than LDA for E_{xc}. Self-interaction corrected functionals, the LDA + U method, and exact-exchange (OEP) functionals proved to be useful for strongly correlated systems. The OEP method in particular (which has been also generalized for time-dependent DFT) is gaining popularity lately.

Most of the quantum ring systems discussed to date are quasi-one-dimensional as it is commonly assumed that the transverse electron motion is confined to the lowest subband. Yet the one-dimensional fermion physics is distinctly different from the common Fermi-liquid picture [20]. The low energy properties are described by the Luttinger-liquid state (for a review see e.g. [21]) where collective excitations replace single-particle excitations of the Fermi liquid. In contrast to two- and three-dimensional systems, it is not possible, to connect adiabatically a non-interacting one-dimensional system to the interacting one, since the ground states of both systems are fundamentally different and even a weak interaction drives the one-dimensional Fermi system into a Luttinger-liquid state. There exist, however, a number of analytically solvable models, such as the Bethe-ansatz solution for the Hubbard model (for a review see [17]) or the bosonization method. With the latter the one-dimensional Wigner crystal has been studied [22]. The specific one-dimensional physics is expected in systems like clean quasi-one-dimensional wires, although it has been shown that impurity scattering restores the Fermi-liquid behaviour [23]. In view of a fundamental difference between the one-dimensional interacting electrons and the Fermi liquid in higher dimensions, it is clear that LDA-type approximations based on the Fermi-liquid-type functionals are not adequate in the one-dimensional case. The applicability of DFT itself is, however, not invalidated, provided the appropriate exchange–correlation functional is used. As such one can use, for example, the LDA functional based on the Bethe-ansatz solution of a Hubbard model [24]. Recently, it has been shown that the Bethe-ansatz-LDA reproduces the key features (e.g. the dispersion of the collective excitations) of the Luttinger liquid, while it fails to describe the scaling of the Drude weight with the system size [25]. This failure, however, is due to the specific form of the LDA and it is unclear whether it affects other functionals as well. As in this paper we do not consider the specific one-dimensional fermion physics but rather focus on the ability of DFT to detect the collective (that is, driven by Wigner crystallization) electron localization, we adopt an OEP

functional which is sufficient for this purpose. Our results show that indeed with only macroscopic variables (current and density) it is possible to observe the collective electron localization entirely within the DFT framework, i.e. not resorting to correlation functions.

As a simple model we consider a ring with a slightly broken rotational symmetry. The symmetry breaking is achieved by introducing a weak localized potential. Calculating the persistent current as a function of the interaction parameter r_S, we find that it stays constant up to the critical value $r_S^c \approx 2.05$ and decays exponentially for larger values of r_S. We interpret this behaviour as a formation of a pinned Wigner crystal at r_S^c. To verify this interpretation we calculate the electron localization function (ELF) [16]. The latter is derived from the local expansion of the pair correlation function and gives a real space picture of the electron localization. We find that below the transition point the ELF corresponds to delocalized electrons whereas it changes to an increasingly localized distribution above the transition point. Taking the amplitude of the electron density oscillations as the order parameter, we find that the system undergoes a second-order phase transition at r_S^c which is reflected by the $(r_S - r_S^c)^{1/2}$ dependence of the order parameter on r_S. The second-order type of transition[1] is a natural consequence of the mean-field character of the theory.

The paper is organized as follows. In section 2 we introduce the model of a one-dimensional quantum ring with the Gaussian impurity potential. We briefly discuss the OEP approximation [26, 27] which is used for the exchange potential. We also introduce an electron localization function (ELF) [16] which is used for a real space visualization of the electron localization. In section 3 we describe the computational method for solving the self-consistent Kohn–Sham equations. In section 4 we present the results for the persistent current as a function of r_S. We consider impurity potentials with different amplitude and width and show how these parameters influence the current. The conclusions are given in section 5.

2. The model

We study a system of $N = 10$ interacting spinless electrons in a quasi-one-dimensional ring of circumference $L = 2\pi R$. The ring geometry is accounted for via periodic boundary conditions and $x = \varphi R$ denotes the coordinate along the ring. Following Friesen and Bergersen [28], we average the electron–electron interaction over the transverse direction. The resulting interaction is well approximated by the function

$$V(x - x') = \frac{e^2}{4\pi\epsilon\epsilon_0} \min\left(|x - x'|^{-1}, a^{-1}\right). \tag{1}$$

We checked that the precise value of the transverse extension of the wire a does not affect our results. A persistent current is induced by a vector potential $\vec{A} = (A_r, A_\varphi)$ with $A_r = 0$ and a tangential component

$$A_\varphi = \frac{\Phi}{L} \tag{2}$$

that provides a magnetic flux Φ through the ring. The vector potential is chosen such that electrons move in a field-free space.

Additionally, we introduce a repulsive Gaussian potential centred at x_0

$$V_{\text{imp}}(x) = V_0 \exp\left(-\frac{(x - x_0)^2}{\sigma^2}\right), \qquad (V_0 > 0) \tag{3}$$

which should pin the Wigner crystal.

We calculate the ground state current density for a given value of magnetic flux and for a given strength and width of the impurity potential using DFT. The self-consistent Kohn–Sham [2] equations for this system are given by

$$\left[\frac{1}{2m_0^*}\left(-\mathrm{i}\hbar\partial_x - eA_\varphi\right)^2 + V_{\text{imp}}(x) + V_{\text{int}}(x)\right]\varphi_i(x) = \epsilon_i\varphi_i(x) \tag{4}$$

where index i labels the Kohn–Sham orbitals φ_i and the eigenvalues ϵ_i. The electron–electron interaction is described by an effective one-particle scalar potential $V_{\text{int}} = V_{\text{H}} + V_{\text{OEP}}^x$. Here, V_{H} is the Hartree potential and V_{OEP}^x is the exchange contribution. The latter is calculated in the Krieger–Li–Iafrate (KLI) version [29, 30] of the OEP method [26, 27].

Commonly, the exchange–correlation energy of the inhomogeneous system is locally approximated by the exchange–correlation energy of a homogeneous system with the respective density. This method is known as the local density approximation (LDA). Since in LDA the exchange–correlation energy of the homogeneous system is given explicitly as a function of the density, the calculation of the exchange–correlation potential as a derivative of the exchange–correlation energy with respect to the density is straightforward. In contrast, in the OEP method the exchange–correlation energy functional is written explicitly in terms of the Kohn–Sham orbitals. A common choice is the 'exact-exchange' functional

$$E_x^{\text{EXX}} = -\frac{1}{2}\frac{e^2}{4\pi\varepsilon\varepsilon_0}\sum_{i,j}^{N}\int \mathrm{d}x \int \mathrm{d}x' \frac{\varphi_i^*(x)\varphi_j(x)\varphi_j^*(x')\varphi_i(x')}{|x - x'|} \tag{5}$$

which has the form of the Fock energy but the wavefunctions φ_i are the Kohn–Sham orbitals rather than the Hartree–Fock orbitals. Unlike LDA, the direct calculation of the derivative of E_x with respect to the density is not possible. Minimization of the total energy functional with respect to the density has to be performed via a chain rule which leads to an integral equation for the exchange potential. In this work we use the exact-exchange functional (5) within the KLI approximation which allows us to transform the OEP integral equation into a considerably simpler algebraic equation. The KLI approximation can be considered as a mean-field approximation to the OEP integral equation,

[1] More rigorously, one can speak of a phase transition only in the thermodynamic limit, which can be approached for very large systems. Our model system of ten electrons is rather a Wigner 'molecule' than a Wigner 'crystal'.

neglecting all terms that vanish after averaging with the density. Substantially simplifying calculations, the KLI approximation retains important features of the exact xc potential such as the derivative discontinuities and the correct asymptotic behaviour [31].

Since DFT in the Kohn–Sham formulation is essentially a mean-field theory, fluctuations are not accounted for in our calculations. It is well known that thermal fluctuations are particularly important in one dimension [20], however, we expect that these fluctuations are effectively suppressed due to the finite size of the ring. Quantum fluctuations are known to be substantial in finite systems [32]. One expects that these fluctuations will smoothen the transition which appears as a sharp cusp in the mean-field DFT calculation. Yet, the two phases away from the transition point—a delocalized electron gas at small r_S and a localized crystal at large r_S—should not be strongly affected.

Whether the ground state of a many electron system is an electron gas-like one or a Wigner crystal state depends on the ratio of the kinetic energy to the Coulomb energy. In one dimension this ratio is simply proportional to the electron density n, whereas in two and three dimensions it is proportional to $n^{1/2}$ and $n^{1/3}$, respectively. Hence for high densities the kinetic energy dominates and the ground state is electron gas-like whereas for low densities the Coulomb repulsion favours the crystalline state.

Experimentally it is most straightforward to vary the electron density to switch between weakly and strongly interacting regimes. Yet the variation of the electron number should alter the persistent current even in a non-interacting system which conceals the interaction effects. As we use a 'persistent current criterion' to identify the Wigner transition we prefer to exclude the aforementioned trivial single-particle contribution and to retain only the influence of many-body effects. It can be done using an alternative (though somewhat artificial) way of controlling the ratio of kinetic and Coulomb energy. Namely, let us consider the electron mass m^* as a free parameter. In one dimension, the parameter r_S is commonly defined as [33]

$$r_S = \frac{1}{2N}\frac{L}{a_B^*}, \tag{6}$$

where L/N is the interelectron distance and

$$a_B^* = 4\pi\varepsilon\varepsilon_0\frac{\hbar^2}{m_0^* e^2} \tag{7}$$

is the Bohr radius, defined with the effective mass m_0^* and dielectric constant ε of the host material. Considering the effective mass as a free parameter we introduce its ratio to the 'true' effective electron mass m^*/m_0^* in the definition of r_S:

$$r_S = \frac{1}{2N}\frac{L}{a_B^*}\frac{m^*}{m_0^*}. \tag{8}$$

The persistent current density

$$j(x) = -\frac{i\hbar}{2m_0^*}\sum_{i=1}^{N}\left[\varphi_i^*(x)\partial_x\varphi_i(x) - \varphi_i(x)\partial_x\varphi_i^*(x)\right] - \frac{\hbar}{m_0^*}\frac{2\pi}{L}\frac{\Phi}{\Phi_0}n(x) \tag{9}$$

should be calculated with the fixed 'true' effective electron mass m_0^*. Here, $\Phi_0 = \frac{h}{e}$ is the flux quantum and

$$n(x) = \sum_{i=1}^{N}\varphi_i^*(x)\varphi_i(x) \tag{10}$$

is the density.

Also, the ratio of the kinetic energy to the impurity potential must be kept constant when changing r_S via changing m^*. Otherwise the current density of a system of non-interacting electrons would depend on r_S. The impurity potential strength V_0 must be renormalized as

$$V_0 \to V_0^* = V_0\frac{m_0^*}{m^*}. \tag{11}$$

The potential renormalization (11) guarantees that the artificial variation of the electron mass results in a dependence of the persistent current on r_S solely due to the electron–electron interaction.

Equation (9) expresses the current density via the Kohn–Sham orbitals within the framework of the ordinary density-based DFT. It is not, however, fully justified since the DFT Kohn–Sham equations by construction yield the exact ground state density but not the current density. Strictly speaking, one has to employ CDFT [34] which expresses the ground state energy functional as a functional of the density and the paramagnetic current density. The Kohn–Sham orbitals in CDFT do give the exact current density of the interacting system. However, a CDFT calculation of the physical current proved redundant for our purposes, as the DFT Kohn–Sham current serves just as well as a localization indicator.

In addition to the Kohn–Sham current, we use the electron localization function (ELF) [16] to visualize the electrons' localization. In the original definition [16] the ELF was invented for real wavefunctions only. Recently it was generalized to the time-dependent case [35] where complex wavefunctions have to be employed. This form of the ELF is also suitable for the current-carrying static system we consider. The idea behind the definition of the ELF is that the localized electron produces a stronger repulsion of the other like-spin electrons (due to the Pauli exclusion principle) than the delocalized one. According to this picture, one calculates the conditional pair probability to find a second electron (with parallel spin) anywhere close to a reference electron. This quantity is expanded in powers of the distance between the electrons: the zeroth-and first-order coefficients vanish because of the Pauli principle and the expansion around a minimum, respectively. The second-order coefficient, normalized to the respective quantity in the homogeneous electron gas, is given by

$$\chi(x) = \frac{\tau(x) - \frac{1}{4}\frac{(n'(x))^2}{n(x)} - \frac{(j_p(x))^2}{n(x)}}{\tau^{\mathrm{hom}}(x)}. \tag{12}$$

In this expression $\tau(x) = \frac{\hbar^2}{m_0^*}\sum_i|\partial_x\varphi_i(x)|^2$ is the kinetic energy density of the Kohn–Sham system and $\tau^{\mathrm{hom}}(x) = \frac{\hbar^2\pi^2}{6m_0^*}n^3(x)$ is the respective quantity in a one-dimensional homogeneous electron gas with density $n(x)$. Physically, $\chi(x)$

is related to the curvature of the exchange hole [36]. In order to restrict the values of the ELF to the interval [0, 1], $\chi(x)$ is not plotted directly. Instead, one defines

$$\eta(x) = \frac{1}{1+\chi^2(x)} \tag{13}$$

which contains the same information as equation (12), but shows a more pronounced structure [16]. For the interpretation of the ELF, two values are of particular importance: its value of one half corresponds to a homogeneous electron gas like state whereas a value of one refers to a completely localized electron at this point in space.

3. Computational method

For numerical solution of the Kohn–Sham equations (4) we use a real space method. We expand the wavefunctions $\varphi_i(x)$ using a spline basis [37]

$$\varphi_i(x) = \sum_\nu a_i^{(\nu)} b_\nu(x) \tag{14}$$

with the complex coefficients $a_i^{(\nu)}$ and the real basis functions

$$b_\nu(x) = \begin{cases} \frac{1}{4}\left(2+\frac{x-x_\nu}{h}\right)^3 : & -2 < \frac{x-x_\nu}{h} \leqslant -1 \\ 1-\frac{3}{2}\left(\frac{x-x_\nu}{h}\right)^2 - \frac{3}{4}\left(\frac{x-x_\nu}{h}\right)^3 : & \\ \qquad -1 < \frac{x-x_\nu}{h} \leqslant 0 & \\ 1-\frac{3}{2}\left(\frac{x-x_\nu}{h}\right)^2 + \frac{3}{4}\left(\frac{x-x_\nu}{h}\right)^3 : & \\ \qquad 0 < \frac{x-x_\nu}{h} \leqslant 1 & \\ \frac{1}{4}\left(2-\frac{x-x_\nu}{h}\right)^3 : & 1 < \frac{x-x_\nu}{h} \leqslant 2 \\ 0: \quad \text{else.} & \end{cases} \tag{15}$$

The spline nodes are x_ν and h is the distance between the two adjacent nodes. The basis functions (15) are not orthogonal which means that the overlap matrix

$$S_{\mu,\nu} = \int \mathrm{d}x\, b_\mu(x) b_\nu(x) \tag{16}$$

is not diagonal. With this representation of the wavefunctions, the Schrödinger equation reads

$$\sum_\nu H_{\mu,\nu} a_i^{(\nu)} = \epsilon_i \sum_\nu S_{\mu,\nu} a_i^{(\nu)} \tag{17}$$

with the Hamiltonian matrix

$$H_{\mu,\nu} = \int \mathrm{d}x\, b_\mu(x) \hat{H} b_\nu(x). \tag{18}$$

At the first step this generalized eigenvalue equation is transformed into a standard eigenvalue equation. We use a Cholesky decomposition [38] of the overlap matrix

$$\hat{S} = \hat{L}\hat{L}^{\mathrm{T}} \tag{19}$$

into a lower triangular matrix $\hat{L}$ and its transpose and write the eigenvalue equation as

$$\hat{L}^{-1}\hat{H}(\hat{L}^{\mathrm{T}})^{-1}\hat{L}^{\mathrm{T}}\vec{a}_i = \epsilon_i \hat{L}^{\mathrm{T}}\vec{a}_i. \tag{20}$$

The matrix $\hat{L}^{-1}\hat{H}(\hat{L}^{\mathrm{T}})^{-1}$ is diagonalized using the `zheev`-routine from the LAPACK library [39] and the resulting eigenvector $\hat{L}^{\mathrm{T}}\vec{a}_i$ is transformed back to obtain the eigenvector $\vec{a}_i$ of the original generalized eigenvalue problem.

The starting point for the iterative self-consistent procedure is a system of non-interacting particles, i.e. a system with $V_{\mathrm{H}} = V^x_{\mathrm{OEP}} = 0$. The resulting non-interacting eigenfunctions are then used to construct the first approximation for the Hartree and the exchange potential. In the subsequent iterations, the Hartree and the exchange potential are calculated from the eigenfunctions of the previous step[2]. As a measure of the convergence we consider the maximum difference between two Kohn–Sham eigenvalues in the nth and $(n-1)$th iteration step:

$$\max_i \left|\varepsilon_i^{(n)} - \varepsilon_i^{(n-1)}\right| < \Delta. \tag{21}$$

We found that this difference has to be extremely small compared to the Kohn–Sham eigenvalues themselves which are of the order of several tens of meV, namely $\Delta \approx 10^{-10}$ meV. The reason for this very small number are low energy excitations which correspond to a charge displacement over a large distance in the system. If the chosen Δ is too large, one encounters a density range where the system seems to be in a delocalized state whereas in fact it becomes localized after the solution is converged. Generally, a very high computational accuracy is required to distinguish correctly between a localized and a delocalized state of the system.

4. Results

In this section we present the results of our calculations of the persistent current in the one-dimensional quantum ring. For the effective electron mass and the dielectric constant we have chosen the GaAs values $m_0^* = 0.0665 m_{\mathrm{e}}$ and $\varepsilon = 12.5$. The value of the magnetic field flux was chosen as $\Phi = 0.3\Phi_0$.

For the Wigner crystal pinning we apply a narrow impurity potential of width $\sigma = 0.025L$ much smaller than the average distance between electrons $\frac{L}{N} = 0.1L$. The persistent current is calculated as a function of r_{S}, the latter being altered by varying m^*, according to equations (8) and (11). The current is normalized to its value j_0 for non-interacting electrons in the presence of an impurity potential with unrenormalized strength $V_0 = 10^{-3}$ meV. The results for various impurity potential strengths are shown in figure 1. The dashed line $\frac{j}{j_0} = 1$ reflects the current independence of r_{S} for non-interacting electrons.

As seen in figure 1 for the smallest $V_0 = 10^{-3}$ meV, one can clearly distinguish two different regions of r_{S}. Below the critical value of $r_{\mathrm{S}}^{\mathrm{c}} \approx 2.05$, the persistent current is independent

[2] To ensure convergence the potential in the nth iteration step is in fact not simply calculated from the density of the previous step. A fraction of the self-consistent potential of the $(n-1)$th step is linearly mixed with it [40]. We used the mixing factor $\alpha = 0.2$.

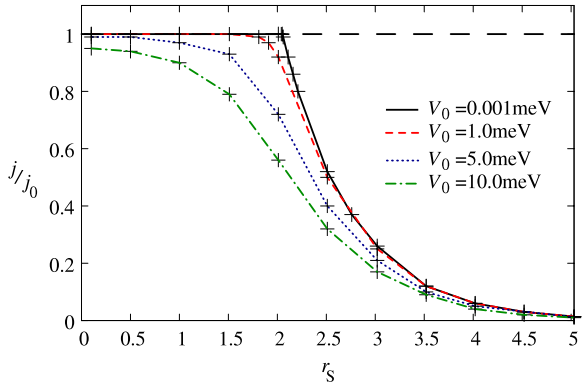

Figure 1. The persistent current as a function of r_S for a Gaussian impurity potential with a half maximum width of 2.5% of the ring circumference. The current is normalized to its value j_0 in a non-interacting system and potential strength $V_0 = 10^{-3}$ meV. The long-dashed line $^{j}/_{j_0} = 1$ corresponds to the interaction-free system.

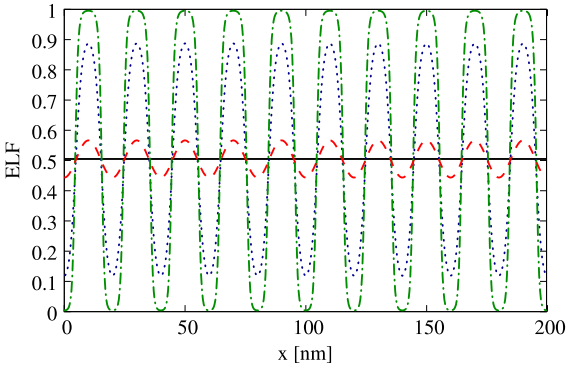

Figure 3. Electron localization function in the presence of a weak ($V_0 = 0.001$ meV) potential. Shown is the ELF for different values of r_S. Solid line: $r_S = 0.1$, dashed line: $r_S = 2.06$, dotted line: $r_S = 2.5$, dash–dotted line: $r_S = 5.0$. An ELF value of one corresponds to perfect localization whereas an ELF value of one half means homogeneous electron gas-like delocalization.

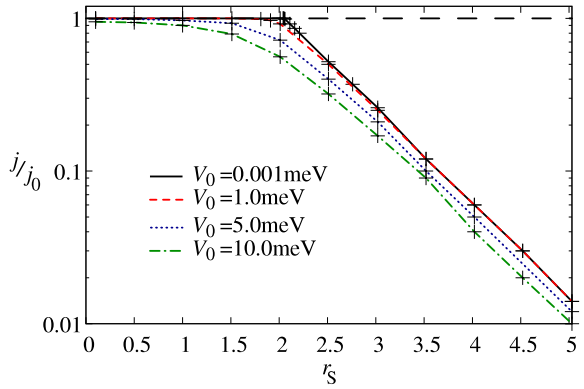

Figure 2. Logarithmic version of the plot in figure 1. The exponential dependence of the persistent current on r_S is clearly seen.

of r_S. Its magnitude is the same as in the non-interacting system which means that the interacting system is electron gas-like. In contrast, for $r_S > r_S^c$, the persistent current drops exponentially with increasing r_S which is seen explicitly from the linear dependence of $\log(j/j_0)$ on r_S shown in figure 2. This signifies the formation of the Wigner crystal pinned by an extremely small impurity potential. Hence the value $r_S^c = 2.05$ can be interpreted as a critical r_S of the Wigner transition in our mean-field model.

This interpretation is supported by the ELF plot in figure 3. For $r_S \leqslant 2.05$ we find an ELF value of one half, corresponding to completely delocalized electrons. This changes drastically when r_S exceeds r_S^c. With increasing r_S the electrons tend to localize at discrete lattice sites. At $r_S \approx 5$ they arrange in an 'almost classical' one-dimensional lattice. The complete localization is achieved within a rather narrow interval of r_S, as exemplified in figure 3 by the ELF graphs for $r_S = 2.06$ and 2.5. This reflects the exponential decay of the persistent current, as shown in figure 1.

We believe, that within our numerical accuracy the solid curve in figure 1 corresponds to the case of the 'vanishing' external potential. Such a potential does not disturb the Wigner transition, but provides the pinning. The particular potential strength and width should then be unimportant. We tested this by calculating the current density for several values of the width of the pinning potential (all with $V_0 = 10^{-3}$ meV) and found that the persistent current follows exactly the same r_S-dependence. However, the convergence is getting much harder for wider potentials since the 'smoother' potentials are less effective in pinning the Wigner crystal. For V_0 values below 10^{-3} meV the convergence could not be reached. Yet using a semiclassical approach [41] it can be shown analytically that the current value j_0 of a non-interacting system is indeed recovered for $V_{\text{imp}} = 0$.

The critical $r_S^c = 2.05$ we obtained in this work is very close to the critical $r_S^{c,\text{discrete}} \approx 2.0$ found in variational calculation for spinless electrons on a discrete one-dimensional ring in the continuum limit [33]. It is also of the same order as the values for r_S^c found in a previous work [40] for a different model using the ground state energy curvature [42] as a localization criterion. In the presence of a disorder potential with an amplitude $\Delta V = 0.02$ meV a Wigner transition has been observed in the range $2.08 \leqslant r_S^c \leqslant 5.04$ depending on the model for the electron–electron interaction.

The other three curves in figure 1 show the current of the interacting system for $V_0 = 1.0$, 5.0 and 10.0 meV. Although at $V_0 = 1.0$ meV there is still the range of r_S where $j = j_0$; the sharp kink at $r_S = r_S^c$ vanishes. The transition smoothing becomes more pronounced in the cases $V_0 = 5.0$ meV and $V_0 = 10.0$ meV where no distinct r_S-independent current regime is seen.

It should be emphasized that the dependence of the normalized current on r_S is solely due to the electron–electron interaction. The smooth decrease of the current with increasingly strong Coulomb interaction observed for stronger impurity potentials ($V_0 = 5.0$ and 10.0 meV) reflects a gradual localization of the many-body state instead of a distinct phase transition. This behaviour parallels the absence of a sharp phase transition in an external potential field that lowers the symmetry of the high-symmetry phase [20].

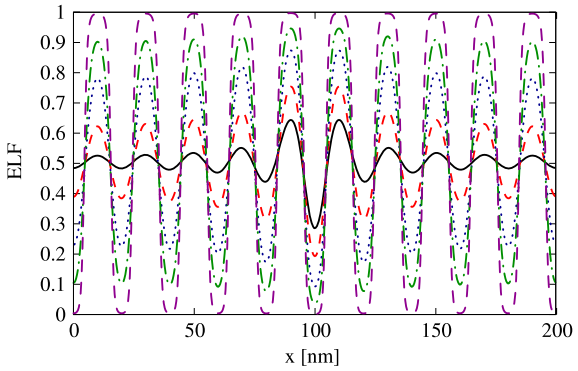

Figure 4. Electron localization function in the presence of an intermediate ($V_0 = 5.0$ meV) narrow potential. Shown is the ELF for different values of r_S. Solid line: $r_S = 0.1$, dashed line: $r_S = 1.5$, dotted line: $r_S = 2.0$, dash–dotted line: $r_S = 2.5$, long-dashed line: $r_S = 5.0$. For intermediate values of r_S the electrons next to the impurity are more localized. This localization increases gradually with increasing r_S. For large values of r_S the ELF is the same as found in the case of the weak potential (see figure 3).

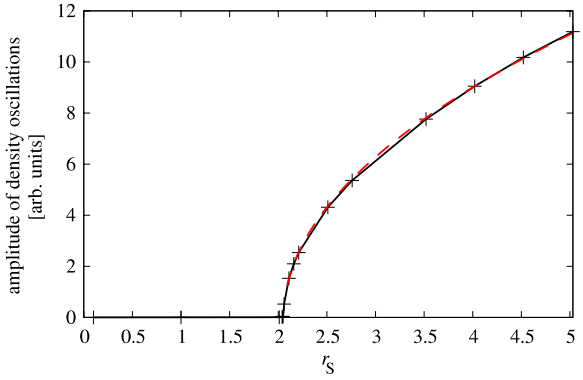

Figure 5. Amplitude of the density oscillations as a function of r_S for a weak impurity potential ($V_0 = 0.001$ meV). The solid black curve shows the calculated data, the dashed red curve is a square root $(r_S - r_S^c)^{1/2}$ behaviour.

An estimate of the Coulomb energy of two electrons at a distance $d = \frac{L}{N} = 20.0$ nm

$$U = \frac{e^2}{4\pi\varepsilon\varepsilon_0}\frac{1}{d} \approx 5.75 \text{ meV} \tag{22}$$

shows that it is indeed of the order of the pinning potential which smoothes out the phase transition and induces a gradual localization. For $V_0 \geqslant 1$ meV and at intermediate values of r_S it can be seen directly from the ELF plots (figure 4) that the localization is more pronounced next to the pinning potential. This indicates that a gradual localization seen in figure 1 is driven by the interplay between the long-range Coulomb repulsion and the interaction with the short-range impurity potential, both being of the same order.

The sharp transition we found for a 'vanishing' impurity potential (solid line in figure 1) is a second-order phase transition from an electron liquid state to the Wigner crystal state. This can be verified by plotting the r_S-dependence of the order parameter δ which shows a behaviour $\delta \sim (r_S - r_S^c)^{1/2}$ at $r_S > r_S^c$, i.e. in the low-symmetry phase [20]. Indeed, taking the amplitude of the density oscillations δn normalized to the average density $n = N/L$ as the order parameter $\delta = \delta n/n$, we obtain an exact square root dependence, as shown in figure 5. The second-order type of the transition we observe in our calculations is quite natural for the mean-field-type DFT-OEP approach.

From the exponential dependence of the current on r_S (figure 1) we can deduce the relation between the persistent current density and the order parameter

$$j(\delta) = j_0 \exp(-\alpha\delta^2) \tag{23}$$

where the numerical factor $\alpha = 3.3$.

5. Conclusions

In this paper we have investigated numerically the influence of the electron–electron interaction on the ground state of a one-dimensional electron gas confined in a ring geometry using the exact-exchange DFT-OEP model. To break the rotational invariance of the ring we introduce a weak 'impurity' potential. This potential does not affect the delocalized electron liquid phase, but provides a pinning of the crystalline Wigner phase. We employ a persistent current in the ring as a measure of the Wigner crystal pinning. For a sufficiently weak impurity potential we found that for $r_S < r_S^c$ the current density of the interacting system is exactly the same as the current density of a non-interacting electron gas. For $r_S > r_S^c$ the current of the interacting system decays exponentially with increasing r_S while the current of a non-interacting system remains constant. This behaviour clearly shows that in the exact-exchange OEP model electron localization via the formation of a Wigner crystal in a one-dimensional system can be achieved. This interpretation is confirmed by the ELF plots which reveal the delocalized electron distribution below the critical r_S^c and a localized one above r_S^c. At $r_S = r_S^c$ the system undergoes a second-order phase transition from an electron liquid to a Wigner crystal. This is evident from the square root dependence of the amplitude of the density oscillations (taken as the order parameter) on r_S above the critical value. Experimentally, this transition should be observable as a decrease of the ring's magnetization when the electron density is lowered. However, in a real experiment this transition will be superposed with the interaction-independent variation of the current density due to the variation of the particle number, and quantum fluctuations are expected to lead to a smooth transition. The critical value $r_S^c = 2.05$ we find for the Wigner transition is consistent with the density range in which Glazman *et al* [43] expected the existence of a stable one-dimensional Wigner crystal.

References

[1] Hohenberg P and Kohn W 1964 *Phys. Rev.* **136** B864–71
[2] Kohn W and Sham L J 1965 *Phys. Rev.* **140** A1133
[3] Dreizler R M and Gross E K U 1990 *Density Functional Theory: an Approach to the Quantum Many Body Problem* (Berlin: Springer)
[4] Runge E and Gross E K U 1984 *Phys. Rev. Lett.* **52** 997
[5] Petersilka M, Gossmann U J and Gross E K U 1996 *Phys. Rev. Lett.* **76** 1212–5

[6] Tokatly I V and Pankratov O 2003 *Phys. Rev.* B **67** 201103
[7] Vignale G 1995 *Phys. Rev. Lett.* **74** 3233–6
[8] Gunnarsson O and Schönhammer K 1986 *Phys. Rev. Lett.* **56** 1968–71
[9] Umrigar C J and Gonze X 1994 *Phys. Rev.* A **50** 3827–37
[10] Wigner E 1934 *Phys. Rev.* **46** 1002–11
[11] Choudhury N and Ghosh S K 1995 *Phys. Rev.* B **51** 2588–91
[12] Tanatar B, Al-Hayek I and Tomak M 1998 *Phys. Rev.* B **58** 9886–9
[13] Tanatar B and Ceperley D M 1989 *Phys. Rev.* B **39** 5005–16
[14] Hamer C J, Quispel G R W and Batchelor M T 1987 *J. Phys. A: Math. Gen.* **20** 5677–93
[15] Schmitteckert P and Werner R 2004 *Phys. Rev.* B **69** 195115
[16] Becke A D and Edgecombe K E 1990 *J. Chem. Phys.* **92** 5397–403
[17] Viefers S, Koskinen P, Singha Deo P and Manninen M 2004 *Physica* E **21** 1–35
[18] Lin J C and Guo G Y 2001 *Phys. Rev.* B **65** 035304
[19] Viefers S, Singha Deo P, Reimann S M, Manninen M and Koskinen M 2000 *Phys. Rev.* B **62** 10668–73
[20] Landau L D and Lifschitz E M 1969 *Course of Theoretical Physics* 2 edn, vol V *Statistical Physics* (London: Pergamon)
[21] Giamarchi T 2004 *Quantum Physics in One Dimension* (*The International Series of Monographs on Physics 121*) 1. publ. edn (Oxford: Clarendon)
[22] Schulz H J 1993 *Phys. Rev. Lett.* **71** 1864–7
[23] Hu B Y-K and Das Sarma S 1993 *Phys. Rev.* B **48** 5469–504
[24] Lima N A, Silva M F, Oliveira L N and Capelle K 2003 *Phys. Rev. Lett.* **90** 146402
[25] Schenk S, Dzierzawa M, Schwab P and Eckern U 2008 *Phys. Rev.* B **78** 165102
[26] Sharp R T and Horton G K 1953 *Phys. Rev.* **90** 317
[27] Talman J D and Shadwick W F 1976 *Phys. Rev.* A **14** 36–40
[28] Friesen W I and Bergersen B 1980 *J. Phys. C: Solid State Phys.* **13** 6627–40
[29] Krieger J B, Li Y and Iafrate G J 1992 *Phys. Rev.* A **45** 101–26
[30] Krieger J B, Li Y and Iafrate G J 1992 *Phys. Rev.* A **46** 5453–8
[31] Grabo T, Kreibich T, Kurth S and Gross E K U 2000 Orbital functionals in density functional theory: the optimized effective potential method *Strong Coulomb Correlations in Electronic Structure Calculations: Beyond the Local Density Approximation* ed V I Anisimov (Amsterdam: Gordon and Breach)
[32] Yannouleas C and Landman U 2007 *Rep. Prog. Phys.* **70** 2067–148
[33] Valenzuela B, Fratini S and Baeriswyl D 2003 *Phys. Rev.* B **68** 045112
[34] Vignale G and Rasolt M 1988 *Phys. Rev.* B **37** 10685–96
[35] Burnus T, Marques M A L and Gross E K U 2005 *Phys. Rev.* A **71** 010501
[36] Dobson John F 1991 *J. Chem. Phys.* **94** 4328–33
[37] Hofmann M, Bockstedte M and Pankratov O 2001 *Phys. Rev.* B **64** 245321
[38] Press W H, Teukolsky S A, Vetterling W T and Flannery B P 1996 *Numerical Recipes in C* (Cambridge: Cambridge University Press)
[39] Anderson E, Bai Z, Bischof C, Blackford S, Demmel J, Dongarra J, Du Croz J, Greenbaum A, Hammarling S, McKenney A and Sorensen D 1999 *LAPACK Users' Guide* (Philadelphia, PA: Society for Industrial and Applied Mathematics)
[40] Hofmann M 2005 Eine *ab initio* Untersuchung der elektronischen Lokalisierung in niederdimensionalen Halbleiterstrukturen mit Wechselwirkung und Unordnung *PhD Thesis* Universität Erlangen-Nürnberg
[41] Krive I V, Sandström P, Shekhter R I, Girvin S M and Jonson M 1995 *Phys. Rev.* B **52** 16451–65
[42] Kohn W 1964 *Phys. Rev.* **133** A171–81
[43] Glazman L I, Ruzin I M and Shklovskii B I 1992 *Phys. Rev.* B **45** 8454–63